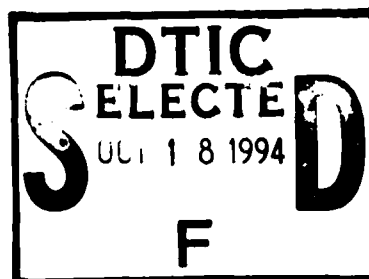


AD-A285 548



1

**MODELING
OPEN BOUNDARY CONDITIONS
BY USING THE
OPTIMIZATION APPROACH**



Building 1103
Stennis Space Center
Mississippi 39529

Phone 601-688-5737
FAX 601-688-7072

by

**Igor Shulman
James K. Lewis**



The University of
Southern Mississippi

TR-1/95

Approved for public release; distribution is unlimited October 1994

6. Comment For ATTN: CHEN DE: 20 Date: 10/10/2010 10/10/2010	J
7.	
8.	
9.	
10.	
11.	
12.	
13.	
14.	
15.	
16.	
17.	
18.	
19.	
20.	
21.	
22.	
23.	
24.	
25.	
26.	
27.	
28.	
29.	
30.	
31.	
32.	
33.	
34.	
35.	
36.	
37.	
38.	
39.	
40.	
41.	
42.	
43.	
44.	
45.	
46.	
47.	
48.	
49.	
50.	
51.	
52.	
53.	
54.	
55.	
56.	
57.	
58.	
59.	
60.	
61.	
62.	
63.	
64.	
65.	
66.	
67.	
68.	
69.	
70.	
71.	
72.	
73.	
74.	
75.	
76.	
77.	
78.	
79.	
80.	
81.	
82.	
83.	
84.	
85.	
86.	
87.	
88.	
89.	
90.	
91.	
92.	
93.	
94.	
95.	
96.	
97.	
98.	
99.	
100.	

1908

94-32350



MODELING OPEN BOUNDARY CONDITIONS BY USING THE OPTIMIZATION APPROACH

I. Shulman

Center for Ocean & Atmospheric Modeling
The University of Southern Mississippi
Stennis Space Center, Mississippi 39529

James K. Lewis

Ocean Physics Research & Development
207 S. Seashore Avenue
Long Beach, Mississippi 39560

ABSTRACT

An optimization approach to prescribe open boundary conditions (OBCs) is proposed. Open boundary conditions are chosen by providing the "best" fit to available observations on the open boundary and to the energy flux through the open boundary. It is shown that many "local" open boundary conditions widely used in the oceanographic community are special cases of the derived optimized OBCs. Numerically, the proposed methods consist of the integration of the governing equations and solving the optimization problem only on the open boundary for each time step. Results of tidal simulations for a channel and the Louisiana-Texas shelf are presented and discussed. Schemes for coupling limited area coastal models with basin scale coarse models by using optimized OBCs are proposed. Preliminary simulations of coupling a fine resolution model of the northern part of the Adriatic Sea and a coarse resolution model of the Mediterranean Sea are presented and discussed. The use of optimized OBCs is shown to be better in predicting tidal amplitudes and phases compared to the use of "local" OBCs.

1. INTRODUCTION

For operational needs of the Navy, coastal nowcast/forecast models will include large open boundaries in the domain of interest because there is no single numerical ocean model which can provide the necessary continuous resolution from the open ocean to the coastal area. The treatment of open boundaries is one of the most interesting problems to be solved while modeling oceanic phenomenon, especially in finite ocean coastal areas. In most ocean models, open boundary conditions (OBCs) are chosen locally, i.e., depending on the solution of the governing equations near the boundary. Many approaches of the local type have been developed (Reid and Bodine, 1968; Orlanski, 1976; Chapman, 1985;

Blumberg and Kantha, 1985; Oey and Chen, 1992 (originally due to Flather, 1976), etc.). The results of numerical studies show that the application of many local-type boundary conditions reproduce the modeled physical phenomenon and work for most practical purposes. However, it is known (Bennett, 1992; Oliger and Sundstrom, 1978) that the local treatment of open boundaries for primitive equation models is an ill-posed problem in that it is difficult to prove that a unique solution exists that is continuously dependent on available observations. Some researchers use the inverse approach to the modeling of open boundary conditions. The open boundary conditions are chosen in such a way as to simultaneously provide the "best" fit to the governing equations

and observations. The "best" fit means the minimization of the norm of the deviation between model results and observations. Thus, the interior solution and available observations are used to calculate variables on the open boundary. This approach has been applied to atmospheric and ocean circulation problems (e.g., Bennett, 1992; Zou et al., 1993; Bogden et al., 1994; Seiler, 1993). The most popular algorithm for solving an inverse problem is an adjoint method in which the initial problem of circulation with open boundary conditions is reduced to integrating the governing equations and an equation for the adjoint variable forward and backward in time (Zou et al., 1993). Although the inverse approach leads to well-posedness, it suffers from a few drawbacks that may restrict its use: requirements for large amounts of computer time and memory and the problem of the stable integration of the adjoint equation. An even more serious problem in using an inverse method is not knowing, *a priori*, the physical properties of the solution. In spite of its "best", the solution may be physically wrong.

There are two major aspects in developing OBCs for coastal models. The first one is to correctly formulate OBCs mathematically and physically for the purpose of reproducing the modeled phenomenon. The second one is to develop necessary techniques for OBCs initialization by the required data. These data can be derived from a) available observations, b) coarse resolution, basin scale model simulations, or c) a combination of a) and b). Initialization can be accomplished by the development of the technology for coupling a coastal model and a basin scale model with the use of data assimilation on the open boundary.

In this paper, we propose methods for modeling open boundary conditions which are based on the integration of the governing equations forward in time and calculating values of variables on the open boundary via a specific inverse problem that provides the "best" fit to available observations on the open boundary and to the energy flux through the open boundary (Shulman and Lewis, 1994). In this way, we avoid the local treatment of the open boundary conditions. All observations on the open boundary and its interior vicinity are used in determining the open boundary conditions for each particular point on the boundary. Numerically, the proposed methods consist of the integration of the governing equations and solving the optimization problem for each time step. We call these open bound-

ary conditions optimized OBCs. We show that some of the well known "local" long-wave radiation boundary conditions which are commonly used in ocean modeling are special cases of the optimized OBCs derived using this approach. The derivations presented here suggest methods for the generation of new boundary conditions based on the requirements of the modeled phenomena.

Most of the approaches to the coupling of basin scale and coastal models can be divided into two groups (Spall and Holland, 1991; Oey and Chen, 1992): "one-way" and "two-way" coupling. In "one-way" coupling, boundary data for a limited area model (LAM) are prescribed by using data from a basin model (usually a coarser resolution, larger domain model). In "two-way" coupling, the evolution within the LAM influences the evolution within the coarser model. We discuss an investigation of "one-way" coupling with the use of our techniques for the specification of OBCs.

2. DERIVATION OF THE OPTIMIZATION PROBLEM

Let P_t be the estimated energy flux through an open boundary, M_t be the estimated mass flux through the same open boundary, F_t be the estimated momentum flux through the open boundary, and vector X be the variables which we should specify on the open boundary (sea surface height, velocity, temperature, salinity, etc.). P_t , M_t , F_t can be estimated by using model values from the interior solution or from simulations from another model (for example, a larger domain, coarse resolution model). Let $J(X)$ be some function of X , $J(X) \geq 0$. We can include available observations and *a priori* information in the specification of $J(X)$. Basically, function $J(X)$ represents the difference between the values of model variables and observations on the open boundary. For each time step we choose open boundary conditions X from the following inverse problem:

$$\min_X J(X), \quad (1)$$

$$A(X) = P_t, \quad (2)$$

$$B(X) = M_t, \quad (3)$$

$$C(X) = F_t, \quad (4)$$

where A, B, C are operators for calculating energy, mass and momentum fluxes. Thus, we choose open boundary conditions by providing the "best" fit to available observations on the open boundary and to the estimated energy, mass, and momentum fluxes through the open boundary. Solving (1)-(4) is a very complicated problem, and different approaches can be used. They all have to take into account that the estimated P_t , M_t , F_t , observations, and *a priori* information in $J(X)$ may contain errors.

In this paper we only consider the solution of (1)-(2) for the vertically-averaged, hydrostatic equations. We introduce the notation

$$P_t = -g \int_S H \eta u_n ds. \quad (5)$$

where S is the open boundary of the model domain D , u_n is the vertically-averaged outward normal velocity, η is the sea surface deviation, H is the depth, and g is the gravitational constant. The term P_t can be interpreted as the flux of total energy penetrating the open boundary S for a model based on the shallow water equations, or as a part of the pressure force work for a vertically-averaged, hydrostatic model. Suppose we estimated the energy flux P_t . We can introduce a criteria to choose one specification of u_n and η which satisfies (5). Consider the following optimization problem:

$$\min_{\eta} J(\eta), \quad (6)$$

constrained by the flux of energy through the open boundary:

$$P_t = -g \int_S H \eta u_n ds. \quad (7)$$

Here $J(\eta)$ is an objective functional depending on η , such that $J(\eta) \geq 0$. Using the Lagrangian method (Fletcher, 1987) to solve the problem (6)-(7), we minimize:

$$\min_{\eta} [J(\eta) - \lambda_t (P_t + g \int_S H \eta u_n ds)]$$

where λ_t is a constant (the Lagrangian multiplier). Thus, the solution of the problem satisfies the following condition:

$$\frac{dJ}{d\eta} - \lambda_t g H u_n = 0. \quad (8)$$

It is important to note that the constant λ_t measures the rate of change in the function $J(\eta)$ due to changes in P_t . Let ϵ_t be the perturbation of P_t : $P^*_t = P_t + \epsilon_t$. It can be shown that (Fletcher, 1987):

$$\lambda_t = -\frac{dJ}{d\epsilon_t}, \quad (9)$$

which provides us with a direct relationship between the various terms of the problem.

3. SOME EXAMPLES OF OPTIMIZED OBCs

In the following, we will show that several of the open boundary conditions used in numerical ocean modeling can be related to the optimization approach of the last section. In each case, a specific objective functional, J , is minimized.

3.1 Simple Longwave Radiation

Let us consider the following problem,

$$\min_{\eta} (J_1 = \frac{g}{2} \int_S \sqrt{gH} \eta^2 ds), \quad (10)$$

with condition (7). In this case, (8) becomes

$$u_n = \frac{\eta}{\lambda_t} \sqrt{\frac{g}{H}}. \quad (11)$$

Note that (11) is the commonly-used long-wave radiation condition with a "tuning" coefficient λ_t which is time dependent. With this coefficient, the relationship given by (11) minimizes the functional $J(\eta)$ given in (10) (in essence, the square of the sea surface height on the open boundary). If $\lambda_t = 1$ (the common radiation condition), then according to (9) we have $dJ/d\epsilon_t = 1$. Under such conditions, we are specifying that the change in the flux of energy penetrating the open boundary will be equal to the change of the functional specified in (10).

3.2 The Reid and Bodine Boundary Condition

There are situations when some extraneous information on the open boundary in the form of

sea surface height, η_T , is available. This information could be direct observations or output of another numerical model. In this case, we can specify the objective functional to be:

$$\min_{\eta} (J_2 = \frac{g}{2} \int_S \sqrt{gH} (\eta - \eta_T)^2 ds), \quad (12)$$

where the model height is fitted to the known function in the least squares sense. In this case, (8) becomes

$$u_n = \frac{(\eta - \eta_T)}{\lambda_t} \sqrt{\frac{g}{H}}. \quad (13)$$

Note that condition (13) is a modified version of that used by Reid and Bodine (1968), which is often used to force regional tidal models while still allowing for the radiation of longwave energy from the interior domain of the model (Lewis et al., 1992). In this case, the relationship given by (13) minimizes the deviation of the sea surface height from the known function η_T (e.g., observed sea surface height variations). When $\lambda_t = 1$, the change in the flux of the energy penetrating the boundary S is equal to the change of the deviation η from η_T .

Oey and Chen (1992) incorporated current velocity information, $u_T(s, t)$, into their open boundary condition (originally due to Flather, 1976). To do so in our formulation, we rewrite (13) in the following form:

$$\sqrt{\frac{g}{H}} (\eta - (\eta_T + \lambda_t \sqrt{\frac{H}{g}} u_{n,T})) = \lambda_t (u_n - u_{n,T}), \quad (14)$$

where $u_{n,T}$ is the outer normal component of the known velocity $u_T(s, t)$. Let us introduce the following notation:

$$\eta^*_{T} = \eta_T + \lambda_t \sqrt{\frac{H}{g}} u_{n,T}. \quad (15)$$

By substituting (15) into (14), we can get the following:

$$u_n - u_{n,T} = \frac{(\eta - \eta^*_{T})}{\lambda_t} \sqrt{\frac{g}{H}}. \quad (16)$$

Condition (16) is a modification of the boundary condition employed by Oey and Chen (1992) with η^*_{T} calculated from (15). The boundary conditions given by (13) and (15)-(16) both minimize the difference between the modeled and observed surface heights [equation (12)]. The difference is that (15)-(16) allows for the inclusion of currents observed at the boundary.

3.3 The Blumberg and Kantha Boundary Condition

We specify the objective functional to be:

$$\min_{\eta} J_3 =$$

$$\frac{g}{2} \int_S \sqrt{gH} [\eta^2 + \frac{1}{\bar{T}} \left(\int_0^t (\eta - \eta_T) dt \right)^2] ds, \quad (17)$$

where \bar{T} is a known constant. The minimization of J_3 subject to the energy flux constraint leads to:

$$\eta - \lambda_t \sqrt{\frac{H}{g}} u_n = -\frac{1}{\bar{T}} \int_0^t (\eta - \eta_T) dt. \quad (18)$$

By differentiation of the equation (18) with respect to t , and after simple transformations we can get the following (Shulman and Lewis, 1994):

$$\frac{\partial \eta}{\partial t} + \lambda_t \sqrt{gH} \frac{\partial \eta}{\partial n} - \frac{d(\lambda_t)}{dt} \sqrt{\frac{H}{g}} u_n = -\frac{1}{\bar{T}} (\eta - \eta_T). \quad (19)$$

The condition specified in (19) is a variation of the boundary condition developed by Blumberg and Kantha (1985) (if $\lambda_t = 1$ for all t). According to (17), condition (19) minimizes the square of η and the deviation of η from η_T over time along the open boundary. If $\bar{T} = t^2$, we are minimizing the square of η and the average deviation of η from η_T over time.

3.4 Some Enhancements

A few simple enhancements of the objective functionals can be considered to derive different open boundary conditions. Consider

$$\min_{\eta} J_4 = \beta_1 J_1 + \beta_2 J_2 =$$

$$\frac{g}{2} \int_S \sqrt{gH} [\beta_1 \eta^2 + \beta_2 (\eta - \eta_T)^2] ds, \quad (20)$$

again with constraint (7). For this case, (8) becomes

$$\beta_1 \eta - \lambda_t \sqrt{\frac{H}{g}} u_n = -\beta_2 (\eta - \eta_T).$$

If $\beta_1 = 1$ and $\beta_2 = \frac{1}{T}$, we have:

$$\eta - \lambda_t \sqrt{\frac{H}{g}} u_n = -\frac{1}{T} (\eta - \eta_T). \quad (21)$$

This formulation provides for the direct specification of u_n at the boundary.

4. DISCUSSION

The optimized open boundary conditions (11), (13), (16), (19), and (21) are not local point wise OBCs, because for calculating λ_t we use data all along the open boundary and its interior vicinity. There are many possible numerical approaches to implementing the proposed boundary conditions. These approaches depend on the numerics of the hydrodynamical model. Here we discuss one of these approaches for the optimized Reid and Bodine boundary condition (13) implemented for a vertically-averaged model. Suppose η_t and $u_{n,t}$ are the sea surface elevation and velocity at time t , and a model uses two previous time steps for calculating variables for the $t+1$ time step. As always, the sea surface elevations η_{t+1} are calculated from the continuity equation, and the velocities u_{t+1} are calculated from the momentum equation. On the open boundary, the following numerical scheme was implemented based on our optimization approach. By using values of η_t and $u_{n,t}$, we can find an estimate of P_t from (5). We have the following optimization problem for time t :

$$\min_{\eta} (J = \frac{g}{2} \int_S \sqrt{gH} (\eta - \eta_{T,t})^2 ds), \quad (22)$$

$$P_t = -g \int_S H \eta u_{n,t} ds. \quad (23)$$

We assume that P_t and $u_{n,t}$ contain some errors in the estimates of the energy flux and the normal velocity. We employ the regularization method (Sabatier, 1987; Parker, 1994) for solving the problem:

$$\min_{\eta} [\frac{1}{2} (P_t + g \int_S H \eta u_{n,t} ds)^2 + \gamma J], \quad (24)$$

where γ is a parameter of regularization. The solution of (24) gives the following expression for λ_t in (13):

$$\lambda_t = -\frac{P_t + g \int_S H \eta_{t,T} u_{n,t} ds}{g^{\frac{1}{2}} \int_S H^{\frac{3}{2}} u_{n,t}^2 ds + \gamma}. \quad (25)$$

After the calculation of λ_t , we rearrange (13) to solve for a corrected value of sea surface elevation at time t using the value of u_n calculated for time t . This corrected value of the sea surface elevation at time t is used for calculating the value of $u_{n,t+1}$

$$u_{n,t+1} = (\eta_t - \eta_{T,t}) \sqrt{\frac{g}{H}}. \quad (26)$$

Because we do not know the norms of the errors in the estimates of P_t and $u_{n,t}$, the parameter γ is chosen in such a way that the two terms in (24) are equal.

5. NUMERICAL EXPERIMENTS

We performed simulations for a flat bottom, frictionless channel which is closed at one end. The channel was forced at the other end by surface oscillations at the M_2 tidal frequency with an amplitude of 1 m. The length of the channel was 355 km. There are 23 grid points along the channel (the 23rd is a wall). We performed simulations for three different values of the channel's depth: 255 m, 1000 m, and 50 m. Figs. 1-3 show the amplitudes and phases of the standing waves based on the analytical solution, a model simulation using the Reid and Bodine boundary condition, and a model simulation using the optimized Reid and Bodine formulation. The use of the optimized Reid and Bodine formulation is seen to eliminate almost entirely errors in the predicted amplitudes while more than halving the errors in the predicted phases.

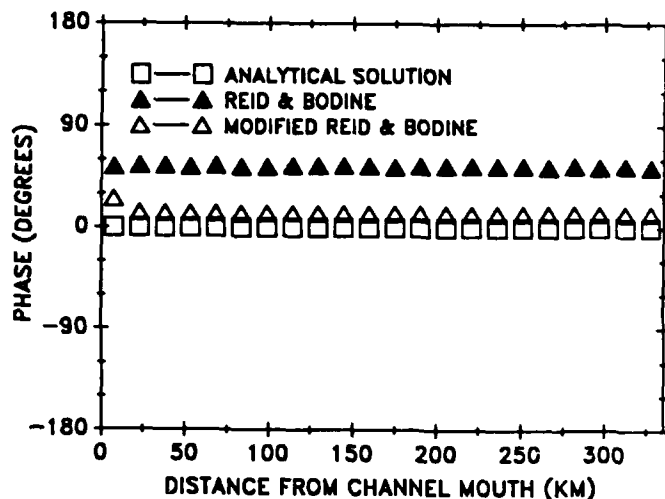
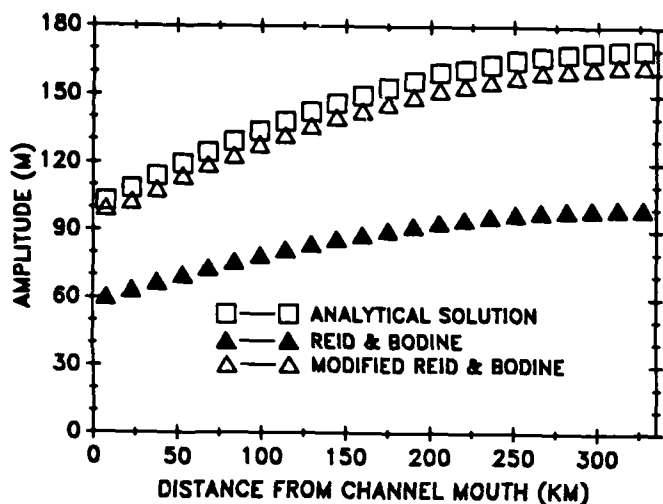


Fig. 1. Amplitude (left) and phase (right) of the standing wave for a 255 m

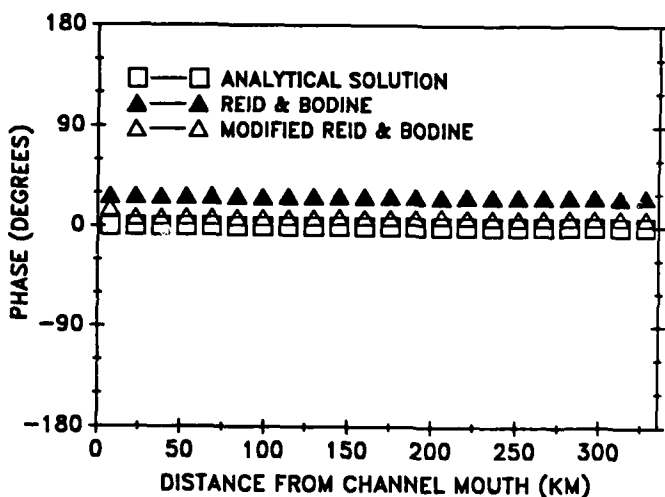
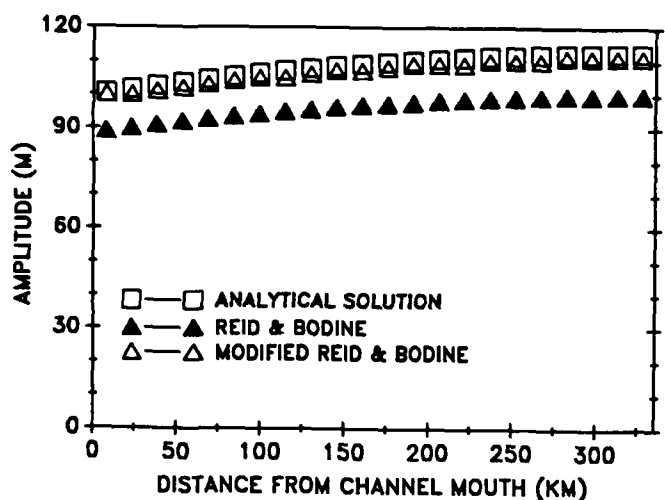


Fig. 2. Same as Fig. 1 but for a 1000 m deep channel.

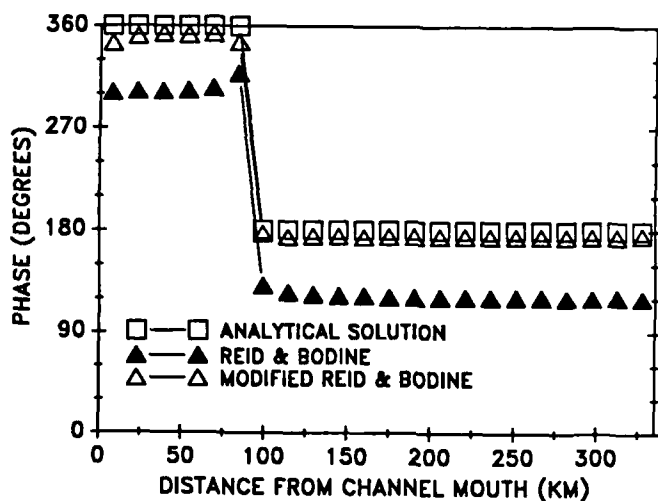
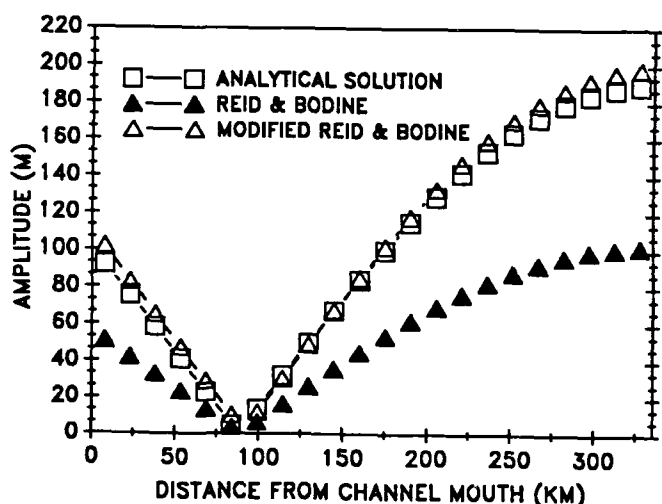


Fig. 3. Same as Fig. 1 but for a 50 m deep channel.

We performed simulations for the M_2 tide over the Louisiana-Texas shelf (LATEX) area (Fig. 4). The model domain has southern and eastern open boundaries, and forcing at these boundaries was determined from the global tide model of Schwiderski (1983). Tables 1 and 2 contain the results of the simulations performed with both the Reid and Bodine and optimized Reid and Bodine conditions [calculating λ_t from (25)]. The use of the optimization approach gives a better prediction of the amplitudes and phases at Galveston, Texas; Port Aransas, Texas; and the weak tide at South West Pass, Louisiana. Fig. 5 shows a comparison between the tidal forcing at the open boundaries and the tides predicted at the model grid cells next to the open boundaries. These results indicate that the modified Reid and Bodine formulation provides a good estimate of the tidal amplitudes, with the largest deviations occurring on the eastern open boundary along the shelf slope. However, the minimization process for this simulation shows a clear bias in overestimating the phases, with the largest overestimates occurring along the southern open boundary.

We also conducted an experiment where the southern and eastern open boundaries were treated separately in our optimization approach. Different values of λ_t were calculated for each open boundary. Thus, the technique would minimize differences along the eastern open boundary independently of those differences along the longer southern open boundary. The results of the simulation are presented in Table 3. In this case, the amplitudes were overestimated and the phases were underestimated. As we mentioned in the introduction, the original Reid and Bodine condition is a local treatment approach to the specification of the open boundary condition: only neighborhood data are used in determining the boundary condition for a grid cell on the boundary. In our approach, all data along and near the boundary are used in calculating the boundary values for each grid point on the boundary, and this approach results in a substantial improvement in predicting amplitudes and phases. However, the separate treatment of the southern and eastern boundaries gives inferior results, likely due to its more "local" treatment of the boundaries.

6. COUPLING TECHNOLOGY AND NUMERICAL EXPERIMENTS

Conditions (13), (16), (19) and (21) can be considered methods of boundary value relaxation toward either observational data or results from a coarser, basin scale model simulation. These conditions have coefficients of relaxation that change in time and provide the adaptation of the boundary conditions to the change in the energy flux through the open boundary. We consider two different schemes for coupling basin and coastal models with the use of data assimilation on the open boundary:

1. providing the "best" fit to the data on the open boundary obtained from observations and/or larger domain, basin model output and to the energy flux generated by an interior solution of a limited area model (LAM),
2. providing the "best" fit to the data on the open boundary obtained from observations and/or larger domain, basin model output and to the energy flux calculated from the basin model.

We tested the first method of coupling by conducting M_2 tidal simulations in the Mediterranean Sea using the explicitly formulated, sigma coordinate version of the Princeton ocean model (Blumberg and Mellor, 1987). Two orthogonal curvilinear grids were used which cover the entire Mediterranean Sea. The first grid had a relatively fine mesh, with a grid size ranging from 4.3 km to 12.3 km and 441x141 grid points in the horizontal. The second grid had a relatively coarse mesh, with a grid size ranging from 3.5 km to 62 km horizontal. All simulations were performed with the bathymetry based on a 2"x2" data base developed by the Naval Oceanographic Office (NAVOCEANO). Direct gravitational M_2 forcing, tidal forcing at the western open boundary, and details about boundary conditions and bottom friction coefficients can be found in Lewis et al. (1994).

The results of the M_2 tidal simulations in the region of the northern Adriatic Sea using the finer grid model are shown in Fig. 6. One can see a good agreement between the model and the observational data from six stations: Porto Piave Vecchia, 45.29°N, 12.34°E; Rovinj, 45.05°N, 13.38°E; Porto Corsini, 44.30°N, 12.17°E; Pesaro 43.55°N, 12.55°E; Ancona, 43.37°N, 13.30°E; and Pula, 44.52°N, 13.50°E. To quantify

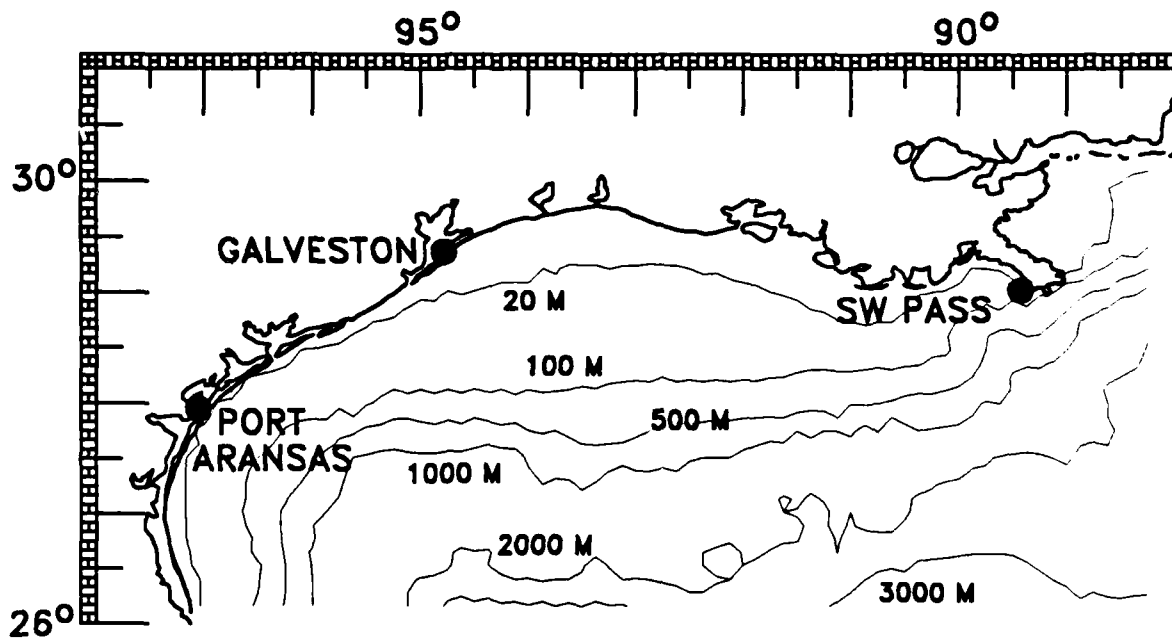


Fig. 4. Model domain and bathymetry (m) for the Texas-Louisiana shelf.

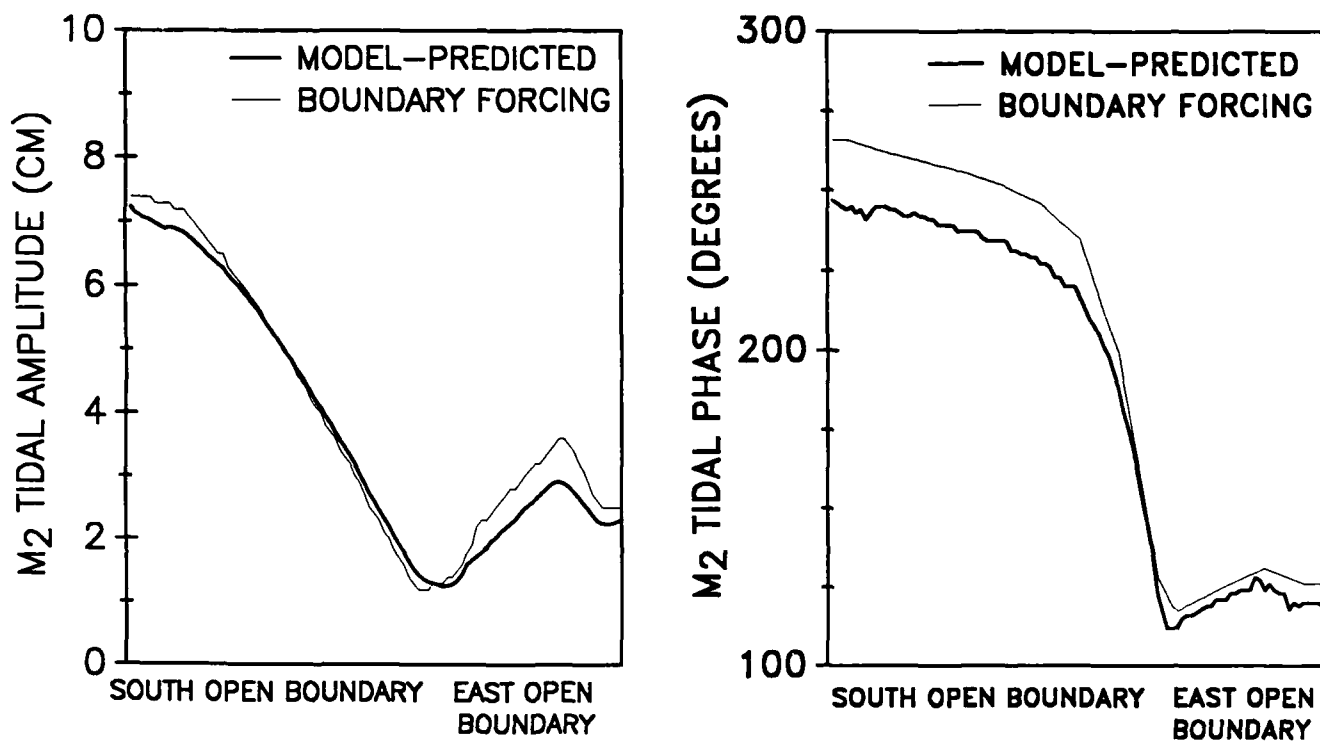


Fig. 5. Amplitude (left) and phase (right) of the M_2 tide along the open boundaries of the LATEX shelf model using the modified Reid and Bodine open boundary formulation.

Table 1. Observed and model-predicted amplitudes (cm.) and phases (degrees, relative to GMT) for the M_2 tide at Galveston, Texas; Port Aransas, Texas; and South West Pass, Louisiana. The model forcing used the standard Reid and Bodine boundary formulation.

Station	Model		Observed	
	Amplitude	Phase	Amplitude	Phase
Galveston	9.1	259.8	13.5	275.1
Port Aransas	6.2	238.0	7.7	262.3
South West Pass	0.2	333.5	1.7	127.2

Table 2. Observed and model-predicted amplitudes (cm.) and phases (degrees, relative to GMT) for the M_2 tide at Galveston, Texas; Port Aransas, Texas; and South West Pass, Louisiana. The model forcing used the optimized Reid and Bodine boundary formulation.

Station	Model		Observed	
	Amplitude	Phase	Amplitude	Phase
Galveston	13.2	262.1	13.5	275.1
Port Aransas	7.9	242.0	7.7	262.3
South West Pass	3.1	136.1	1.7	127.2

Table 3. Observed and model-predicted amplitudes (cm.) and phases (degrees, relative to GMT) for the M_2 tide at Galveston, Texas; Port Aransas, Texas; and South West Pass, Louisiana. The model forcing used the optimized Reid and Bodine boundary formulation for the eastern open boundary and again for the southern open boundary.

Station	Model		Observed	
	Amplitude	Phase	Amplitude	Phase
Galveston	15.4	251.0	13.5	275.1
Port Aransas	9.6	234.2	7.7	262.3
South West Pass	8.1	120.5	1.7	127.2

the errors, we calculated a weighted average percent error for these six northern Adriatic Sea stations. The weighting is the respective tidal amplitudes at each station. Thus, the errors at stations with relatively small tidal amplitudes do not influence the average error as much as errors at stations with larger amplitudes. The average weighted error for the prediction of amplitudes using the finer grid model is about 16%. The prediction of the M_2 tides in the northern Adriatic using the coarser grid model (Fig. 6) are considerably worse, with percent errors reaching as high as 166%. It is clear that the M_2 tidal prediction in the northern Adriatic using this coarser resolution model is relatively poor.

To simulate the tides in the northern part of the Adriatic Sea only, a third, limited area model (LAM) was produced. The LAM was based on a portion of the mesh of the finer grid Mediterranean Sea model (same grid location and resolution; see Fig. 7). The open boundary for the LAM was placed between points with coordinates 42.53°N, 13.57°E and 44.56°N, 14.32°E (Fig. 7). The bathymetry for the LAM ranged from 2.3 m to 80 m. The LAM was coupled with the coarse grid model by using scheme 1 and using the optimized Reid and Bodine OBC in (13).

In the first coupling experiment, the amplitudes and phases of the sea surface elevation from the coarse grid simulation were interpolated to

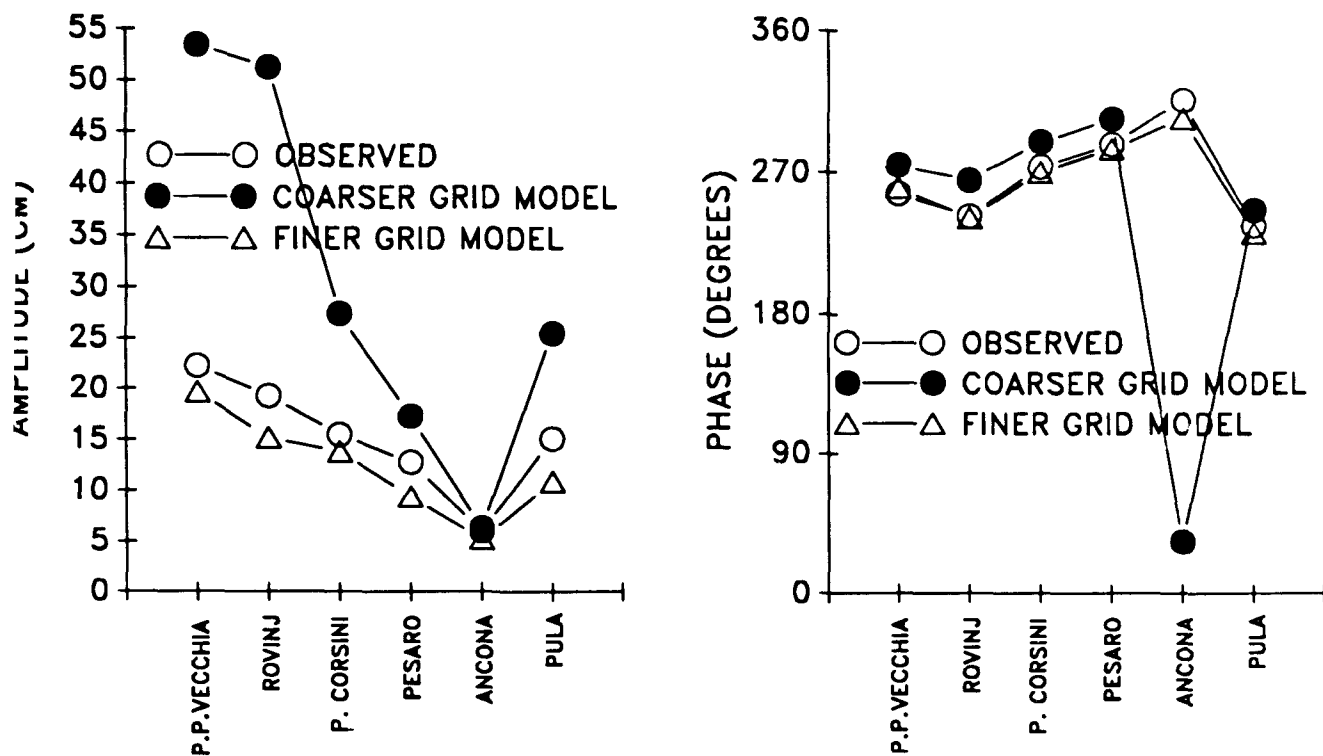


Fig. 6. Observed and model-predicted amplitudes and phases (relative to GMT) for the M_2 tide in the northern Adriatic Sea based on a simulation using the fine and the coarser grid models of the Mediterranean Sea.

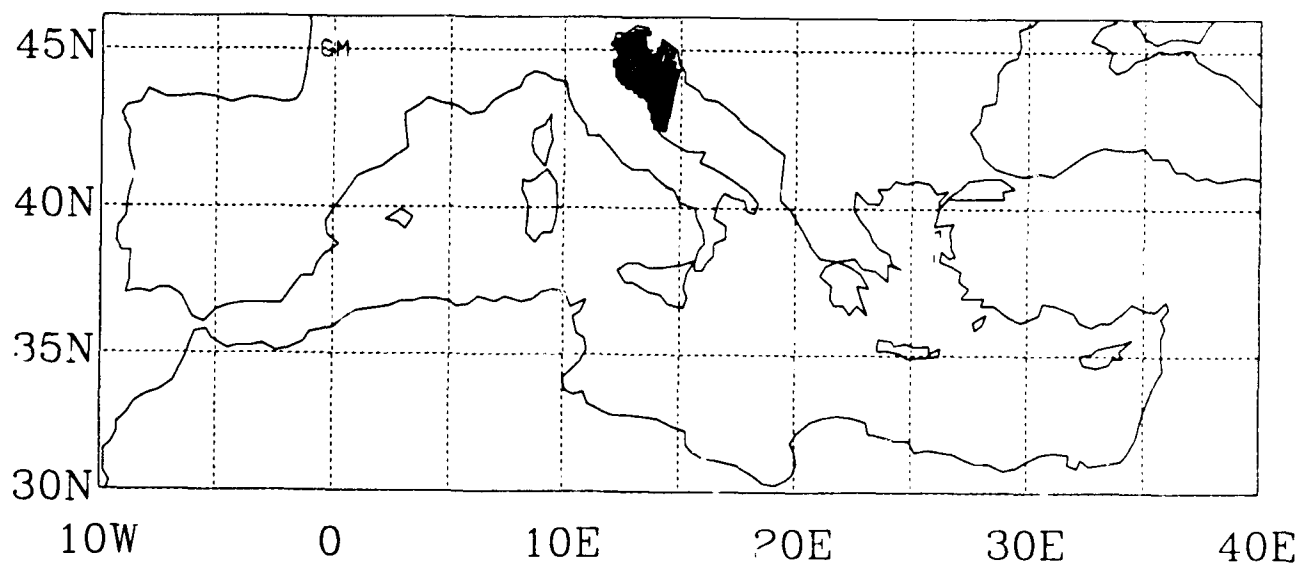


Fig. 7. Limited area model (LAM) of the northern part of the Adriatic Sea.

the open boundary of the LAM and used as η_T in (13). We conducted coupling tests with $\lambda_t = 1$ in (13) (standard Reid and Bodine) and with our optimized approach where λ_t is calculated for each time step. The results are shown in Fig. 8. One can see that the use of the standard Reid and Bodine boundary condition underestimated the amplitudes by up to 50%. The results of simulations with the optimized OBC showed better agreement with the observations, but some amplitudes were overestimated. The average weighted error was around 10%, relatively good considering that the coarse resolution model output was used to force the model.

In our experiments, we placed the open boundary of the LAM in such a way that another tidal station, Porto Cigale (44.32°N, 14.27°E), lies on the open boundary. For the second experiment, the amplitude and phase of η_T were equal to the amplitude and phase of the Porto Cigale station for each grid cell on the open boundary of the LAM. The results of the simulation are shown in Fig. 9 for the Reid and Bodine and optimized open boundary conditions, respectively. The results are inferior for both open boundary conditions compared to the first experiment. Obviously, the observational data of the one station is not enough to force the limited area model properly.

For the third coupling experiment, we combined the output of the coarse grid run and the data of the Porto Cigale station to create η_T . For the open boundary points close to Porto Cigale, the values of η_T were equal to that station's data. For the remaining grid points, the values of η_T were the same as in first experiment; i.e., interpolated from the output of the coarser grid simulation. The results of the LAM simulations are shown in Fig. 10. Again, the standard Reid and Bodine boundary condition produced percent errors on the order of 50% in the prediction of amplitudes. Using the optimization technique, the LAM predictions had a weighted average error of 10% for the amplitudes and 1.7% for the phases. It would appear that forcing the model with optimized OBCs and using both observations and the results from the coarser model simulation produces results that are even better than those of the finer grid model of the entire Mediterranean Sea (Fig. 6). Additional research of this phenomena is being pursued.

7. CONCLUSIONS AND FUTURE PLANS

As we have shown, many of the familiar formulations used as open boundary conditions in barotropic numerical simulations can have certain optimization properties based on the coefficient λ_t . This coefficient allows the adaptation of the boundary condition to the change in the flux of energy penetrating the open boundary as well as the minimization of differences between observations and predictions. By choosing the appropriate functional to minimize along the open boundary, the proposed approach allows a modeler to generate different types of boundary conditions based on *a priori* information and the inclinations of the modeler. Optimized OBCs can be considered as data assimilation schemes, where functions η_T , $u_T(s, t)$ and P_t include *a priori* information of the phenomenon being modeled.

The results of simulations showed that the proposed optimized OBCs for a barotropic model work very well in reproducing tidal phenomenon and can be used in coupling coarse resolution, basin scale models with fine resolution, limited area models. We plan to extend our approach to the modeling of three-dimensional open boundary conditions and developing techniques for coupling basin and coastal models by using optimized OBCs.

ACKNOWLEDGMENTS

We would like to thank Drs. R. Passi and A. Blumberg for excellent and encouraging comments. This work was supported by a research grant from the Office of Naval Research to the Center for Ocean & Atmospheric Modeling, The University of Southern Mississippi.

REFERENCES

- Bennett, A., 1992: *Inverse Methods In Physical Oceanography*. Cambridge Univ. Press, 346 pp.
- Blumberg, A., and L. Kantha, 1985: Open boundary condition for circulation models. *J. Hydro. Eng.*, 111, 2, 237-255.
- Blumberg, A., and G. L. Mellor, 1987: A description of a three-dimensional coastal ocean circulation model. In: *Three Dimensional Coastal Models*, N.S. Heaps (ed.). Coastal and Estuarine

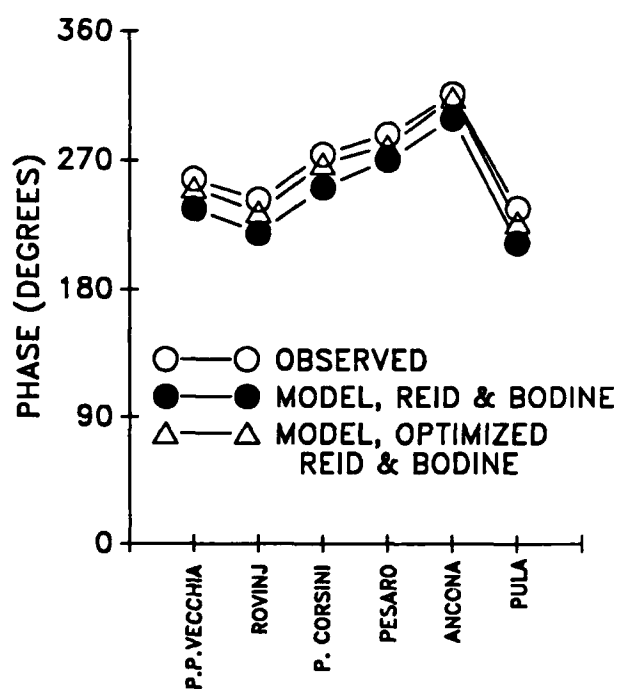
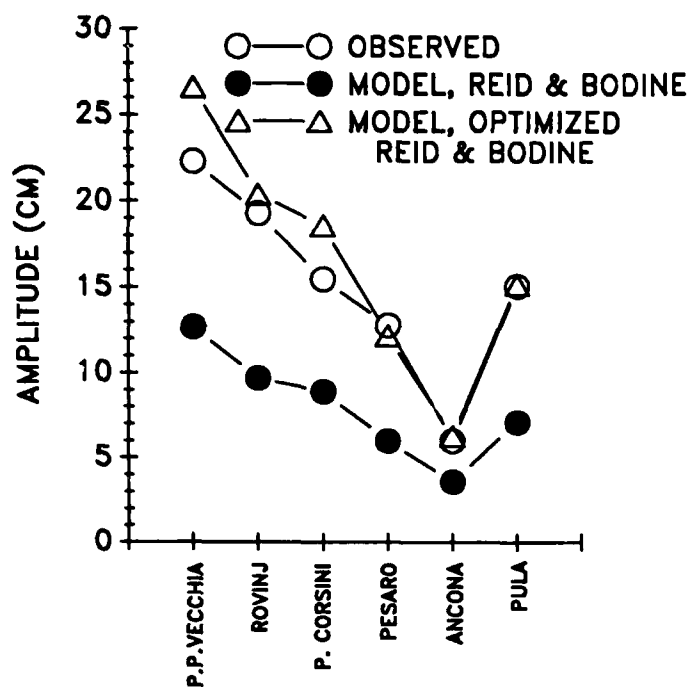


Fig. 8. Observed and model-predicted amplitudes and phases (relative to GMT) for the M_2 tide based on a simulation using a limited area model of the northern Adriatic Sea. The model forcing used the interpolated output from the coarser grid Mediterranean Sea model and the standard and the optimized Reid and Bodine boundary formulation.

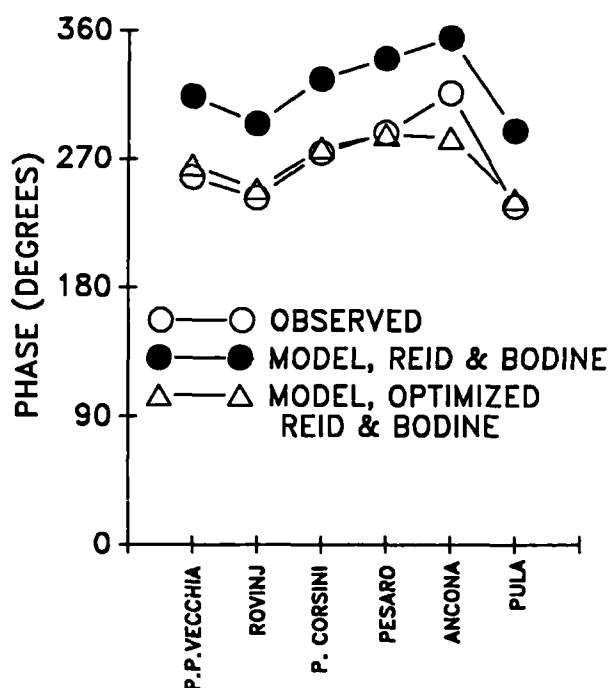
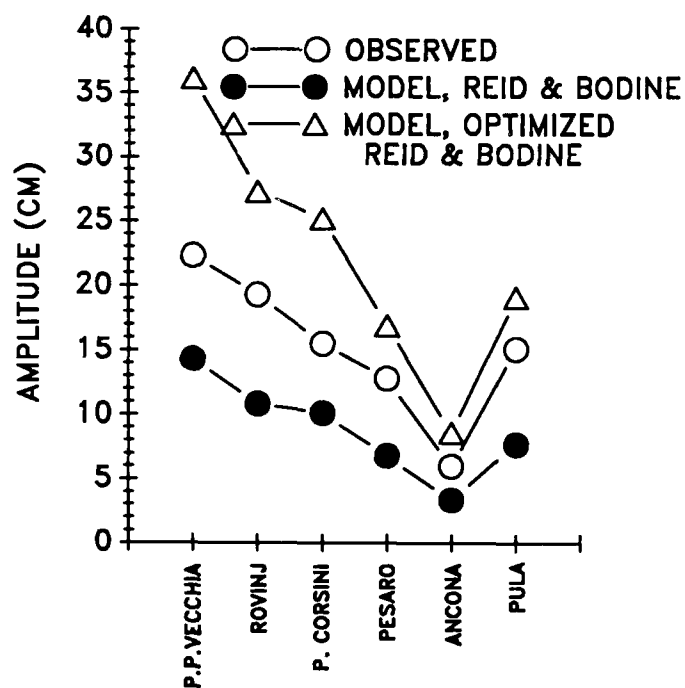


Fig. 9. Same as Fig. 8 but the model forcing used the Porto Cigale station's data.

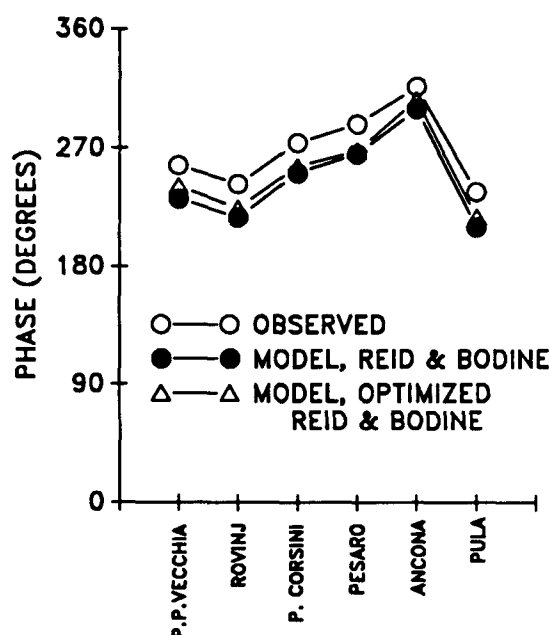
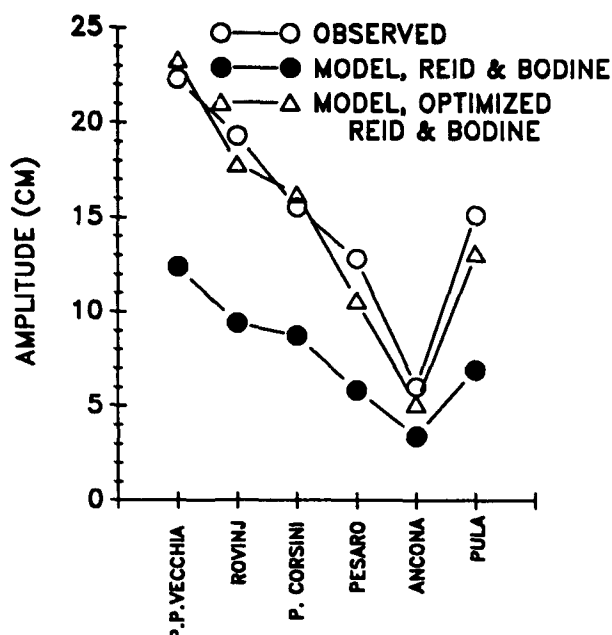


Fig. 10. Same as Fig. 8 but the model forcing used the interpolated output from the coarser grid Mediterranean Sea model plus the observed data from Porto Cigale station.

Sciences, 4, Am. Geophys. Un., 1-16.

Bogden, P. S., P. Malanotte-Rizzoli, and R. P. Signell, 1994: Open-ocean boundary conditions from interior data: local and remote forcing of Massachusetts Bay. *EOS, Trans. of the Am. Geophys. Un.*, Vol. 75, , 3, p. 80.

Chapman, D., 1985: Numerical treatment of cross-shelf open boundaries in a barotropic coastal ocean model. *J. Phys. Oceanogra.*, 15, 1060-1075.

Flather, R. A., A tidal model of the north-west European continental shelf. *Mern. Soc. R. Sci. Liege, Ser. 6*, 10, 141-164, 1976.

Fletcher, R., 1987: *Practical Methods Of Optimization*. John Wiley and Sons, New York, 436 pp.

Lewis, J., G. Vayda, and Y. Hsu, 1992: Coupling regional and global tide models. *J. Mar. Tech. Soc.*, 26, 2, 78-87.

Lewis, J., R. Passi, I. Shulman, and E. Fu., 1994: Simulation experiments using a fine-grid hydrodynamic model of the Mediterranean Sea. Report to the Office of Naval Res., Center for Ocean & Atmosph. Modeling, The Univ. of South. Miss., 19 pp.

Oey, L.-Y., and P. Chen, 1992: A model simulation of circulation in the north-east Atlantic shelves and seas. *J. Geophys. Res.*, 97, 20087-20115.

Oliger, J., and A. Sundstrom, 1978: Theoretical and practical aspects of some initial boundary value problems in fluid dynamics, *SIAM*

J. Appl. Math., 35(3), Nov., 419-446.

Orlanski, I., 1976: A simple boundary condition for unbounded hyperbolic flows. *J. of Comput. Phys.*, 21, 251-269.

Parker, R. L., 1994: *Geophysical Inverse Theory*. Princeton Press, 386 pp.

Reid, R. O., and B. R. Bodine, 1968: Numerical model for storm surges in Galveston Bay. *ASCE, J. Water. and Harb. Div.*, 94, 33-57.

Sabatier, P.C., editor, 1987: *Basic Methods of Tomography and Inverse Problems*. Adam Hilger, Bristol and Philadelphia, 671 pp.

Seiler, U., 1993: Estimation of the open boundary conditions with the adjoint method. *J. Geophys. Res.*, 98(C12), 22855-22870.

Shulman, I., and J. Lewis, 1994: Optimization approach to the treatment of open boundary conditions. In press, *J. Phys. Oceanogra.*

Spall, M. A., and W. R. Holland, 1991: A nested primitive equation model for oceanic applications. *J. Phys. Oceanogra.*, 21, 2, 205 -220.

Schwiderski, E. W., 1983: Atlas of ocean tidal charts and maps, Part I: the semidiurnal principal lunar tide M_2 . *Mar. Geodesy*, Vol. 6, 219-265.

Zou, X., I. M. Navon, M. Berger, P. K. Phua, T. Schlick, and F. X. LeDimet, 1993: Numerical experience with limited memory quasi-Newton methods for large-scale unconstrained nonlinear minimization. *SIAM J. on Optimization*, 3, No. 3, 582-608.

DISTRIBUTION LIST

Administrative Grants Officer (1)
Office of Naval Research
Atlanta Regional Office
101 Marietta Tower
Tower Suite 2805
101 Marietta Street
Atlanta, GA 30323

Director, Naval Research Laboratory (1)
Attn: Code 2627
Washington, D. C. 20375

Defense Technical Information Center (2)
Building 5, Cameron Station
Alexandria, VA 22304-6145

Office of Naval Research
Ballston Centre Tower One
800 North Quincy Street
Arlington, VA 22217-5000

Ed Chaika
Manuel Fiadeiro
Thomas Kinder
Robert Peloquin (3)
Rick Spinrad
Alan Weinstein

Code 7000
Naval Research Laboratory
Washington, D. C. 20375-5320
Eric Hartwig

U. S. Geological Survey, WRD
345 Middlefield Road, MS-496
Menlo Park, CA 94025
Ralph T. Cheng

Naval Oceanography Command
Building 1020
Stennis Space Center, MS 39529
Don Durham

Naval Oceanographic Office
Stennis Space Center, MS 39529
Charles Horton

Naval Research Laboratory
Stennis Space Center, MS 39529
George Heburn
Larry Hsu
Harley Hurlburt
Paul Martin
Joe McCaffrey
Steve Piacsek
Ruth Preller

Department of Oceanography
Naval Postgraduate School
Monterey, CA 93943
Peter Chu
Ly Ngoc Le

Department of Oceanography
Old Dominion University
Norfolk, VA 23529-0276
A. D. Kirwan

Princeton University
P. O. Box CN710, Sayre Hall
Princeton, NJ 08544-0710
Kirk Bryan
Peter Chen
Tal Ezer
George Mellor

Mesoscale Air-Sea Interaction
Group
B-174, 020 Love Building
The Florida State University
Tallahassee, FL 32306-3041
James J. O'Brien

Harvard University
29 Oxford Street, Room 100D
Cambridge, MA 02138
Allan R. Robinson

Oregon State University
College of Oceanic & Atmospheric
Sciences
Corvallis, OR 97331-2879
John Allen
Andrew Bennett

Rutgers University
P. O. Box 231
New Brunswick, NJ 08903-0231
Dale Haidvogel

Woods Hole Oceanographic Institution
Woods Hole, MA 02543
Dave Chapman

University of Colorado
Campus Box 431
Boulder, CO 80309-0431
Lakshmi Kantha

Texas A & M University
Department of Oceanography
College Station, TX 77843
Robert Reid

NOAA Great Lakes Environmental
Research Laboratory
2205 Commonwealth Boulevard
Ann Arbor, MI 48105
William O'Connor

Massachusetts Institute of
Technology
Department of Earth Atmospheric
and Planetary Sciences
Cambridge, MA 02139
Paola Rizzoli
Carl Wunsch

Los Alamos National Laboratory
Los Alamos, NM 87545
C. Aaron Lai

Dept. of Civil, Environmental
and Coastal Engineering
Stevens Institute of Technology
Hoboken, NJ 07030
Lie-Yauw Oey

University of Miami/RSMAS
4600 Rickenbacker Causeway
Miami, FL 33149-1098
Dong-Shan Ko
Christopher N. K. Mooers

HydroQual, Inc.
1 Lethbridge Plaza
Mahwah, NJ 07430
Alan Blumberg
Kirk Ziegler

Mississippi State University
Department of Civil Engineering
P. O. Drawer CE
Mississippi State, MS 39762
Adnan Shindala
Victor L. Zitta

School of Mathematical Sciences and the
Scientific Computing Program
The University of Southern Mississippi
Building 1103, Room 103
Stennis Space Center, MS 39529
A. Louise Perkins
Grayson Rayborn

Dr. Denis Wiesenburb, Director
Center for Marine Sciences
The University of Southern Mississippi
Building 1103, Room 102
Stennis Space Center, MS 39529

Dr. Stephen A. Doblin, Dean
Science and Technology
The University of Southern Mississippi
Southern Station Box No. 5165
Hattiesburg, MS 39406-5165

Dr. Karen M. Yarbrough
Vice President for Research and
Planning
The University of Southern Mississippi
Southern Station Box No. 5116
Hattiesburg, MS 39406-5116

Center for Air Sea Technology
Mississippi State University
Building 1103, Room 233
Stennis Space Center, MS 39529
Jim Corbin
David Dietrich

REPORT DOCUMENTATION PAGE

Form Approved
OMB No. 0704-0188

Public reporting burden for this collection of information is estimated to average 1 hour per response, including the time for reviewing instructions, searching existing data sources, gathering and maintaining the data needed, and completing and reviewing the collection of information. Send comments regarding this burden estimate or any other aspect of this collection of information, including suggestions for reducing this burden, to Washington Headquarters Services, Directorate for Information Operations and Reports, 1215 Jefferson Davis Highway, Suite 1204, Arlington, VA 22202-4302, and to the Office of Management and Budget, Paperwork Reduction Project (0704-0188), Washington, DC 20503.

1. Agency Use Only (Leave blank).		2. Report Date. October 1994		3. Report Type and Dates Covered. Technical Report	
4. Title and Subtitle. MODELING OPEN BOUNDARY CONDITIONS BY USING THE OPTIMIZATION APPROACH				5. Funding Numbers. Program Element No. Project No. Task No. Accession No.	
6. Author(s). Igor Shulman James K. Lewis					
7. Performing Organization Name(s) and Address(es). Center for Ocean & Atmospheric Modeling The University of Southern Mississippi Building 1103, Room 249 Stennis Space Center, MS 39529-5005				8. Performing Organization Report Number. TR-1/95	
9. Sponsoring/Monitoring Agency Name(s) and Address(es). Office of Naval Research Code 1513: RKL Ballston Centre Tower One 800 North Quincy Street Arlington, VA 22217-5660				10. Sponsoring/Monitoring Agency Report Number.	
11. Supplementary Notes. ONR Research Grant No. N00014-92-J-4112					
12a. Distribution/Availability Statement. Approved for public release; distribution is unlimited.				12b. Distribution Code.	
13. Abstract (Maximum 200 words). An optimization approach to prescribe open boundary conditions (OBCs) is proposed. Open boundary conditions are chosen by providing the "best" fit to available observations on the open boundary and to the energy flux through the open boundary. It is shown that many "local" open boundary conditions widely used in the oceanographic community are special cases of the derived optimized OBCs. Numerically, the proposed methods consist of the integration of the governing equations and solving the optimization problem only on the open boundary for each time step. Results of tidal simulations for a channel and the Louisiana-Texas shelf are presented and discussed. Schemes for coupling limited area coastal models with basin scale coarse models by using optimized OBCs are proposed. Preliminary simulations of coupling a fine resolution model of the Mediterranean Sea are presented and discussed. The use of optimized OBCs is shown to be better in predicting tidal amplitudes and phases compared to the use of "local" OBCs.					
14. Subject Terms. OPEN BOUNDARY CONDITIONS (U), LIMITED AREA MODELS (U), DATA ASSIMILATION (U), COUPLING TECHNIQUES (U)				15. Number of Pages. 21	
				16. Price Code.	
17. Security Classification of Report. Unclassified	18. Security Classification of This Page. Unclassified	19. Security Classification of Abstract. Unclassified	20. Limitation of Abstract. SAR		